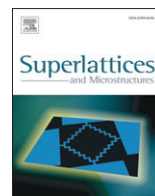




ELSEVIER

Contents lists available at ScienceDirect

Superlattices and Microstructures

journal homepage: www.elsevier.com/locate/superlattices

Low-temperature growth and properties of flower-shaped β -Ni(OH)₂ and NiO structures composed of thin nanosheets networks

A. Al-Hajry^{a,*}, Ahmad Umar^b, M. Vaseem^b, M.S. Al-Assiri^c, F. El-Tantawy^c, M. Bououdina^d, S. Al-Heniti^e, Y.-B. Hahn^b

^a Department of Physics, College of Science, Najran University, P. O. Box 1988, Saudi Arabia

^b School of Semiconductor and Chemical Engineering and BK21 Centre for Future Energy Materials and Devices, Chonbuk National University, Jeonju, 561756, South Korea

^c Department of Physics, College of Science, King Khalid University, P.O. Box 9003, Abha, Saudi Arabia

^d Department of Physics, College of Science, University of Bahrain, P.O. Box 32038, Kingdom of Bahrain

^e Department of Physics, Faculty of Science, King Abdul Aziz University, Saudi Arabia

ARTICLE INFO

Article history:

Received 11 March 2008

Received in revised form

13 April 2008

Accepted 22 April 2008

Available online 11 June 2008

Keywords:

β -Ni(OH)₂

NiO

Nanosheet networks

Solution process

Thermogravimetric studies

ABSTRACT

Flower-shaped β -Ni(OH)₂ structures composed of thin nanosheet networks have been synthesized via the simple aqueous solution route by using nickel chloride and ammonium hydroxide at 65 °C in 4 h. The general morphological observations revealed that the flowers are composed of thin nanosheets which were connected to each other in such a manner that they form network-like morphologies. Moreover, single-crystalline flower-shaped NiO structures composed of thin nanosheets were also obtained by thermal decomposition of flower-shaped β -Ni(OH)₂ structures. The shape of nanosheet networks in β -Ni(OH)₂ was sustained after thermal decomposition to NiO however, some broken nanosheets were also observed from the flower-shaped structures of NiO. The as-prepared products were characterized by X-ray powder diffraction (XRD), field emission scanning electron microscope (FESEM), transmission electron microscope (TEM), high-resolution TEM (HRTEM), Fourier transform infrared spectroscopy (FTIR), and Thermogravimetric analysis (TGA).

© 2008 Elsevier Ltd. All rights reserved.

* Corresponding author. Tel.: +966 75441849; fax: +966 75442135.
E-mail address: ahajry@gmail.com (A. Al-Hajry).

1. Introduction

Nickel hydroxide ($\text{Ni}(\text{OH})_2$), as one of the most important transition metal hydroxides, has received increasing attention due to its exotic properties and extensive applications, especially as a positive electrode active material, in alkaline rechargeable nickel-based batteries, with characteristics of high power density, excellent cyclability, high specific energy and low toxicity [1]. As far as nickel oxide (NiO) is concerned, it is *p*-type wide-band-gap material which can be used as a transparent *p*-type semiconducting layer [2]. As an important material, NiO can be used in various applications, such as magnetic materials, catalysts, electrochromic films, fuel cell electrodes, gas sensors, active optical fibers, battery electrodes etc [3–5]. It has been observed that the performance of alkaline rechargeable nickel-based batteries and other devices depends on the structural and morphological features of $\text{Ni}(\text{OH})_2$ and NiO , hence considerable work has been done to prepare and investigate nanocrystalline $\text{Ni}(\text{OH})_2$ and NiO nanostructures [1–7]. Previously reported results on the synthesis of nickel hydroxide and NiO , mostly, were done either at higher temperature and pressure or by using expensive instruments (autoclaves) and chemicals. Therefore, it is desirable to explore simple and low-cost methods for the large-scale production of $\text{Ni}(\text{OH})_2$ and NiO nanostructures to fulfill the high demands of these kinds of materials for their effective use in various applications such as battery materials, sensors, fuel cells etc.

In this paper, we present a very simple and effective aqueous solution route to synthesize the good quality in large-quantity flower-shaped β - $\text{Ni}(\text{OH})_2$ and NiO nanostructures composed of nanosheet networks by using nickel chloride and ammonium hydroxide at 65 °C in 4 h. The flowers of β - $\text{Ni}(\text{OH})_2$ with high-specific surface area are promising positive electrode materials for alkaline rechargeable batteries. Moreover, these structures can also be used as a starting material for the synthesis of NiO nanostructures, widely used and versatile materials for the fabrication of catalysts, sensors, and electrochemical devices. The as-synthesized products were characterized in detail by XRD, FESEM, HRTEM, FTIR, and TGA.

2. Experimental details

2.1. Experiment procedure

All the reagents used in this synthesis were in analytical grade and used as received without further purification. The typical reaction process for the synthesis of flower-shaped β - $\text{Ni}(\text{OH})_2$ nanostructures was as follows: 0.025 M $\text{NiCl}_2 \cdot 6\text{H}_2\text{O}$ solution prepared in 50 ml of deionized (DI) water which was then heated up to 65 °C under continuous stirring. Subsequently, 7 M aqueous solution of ammonium hydroxide (NH_4OH) was added drop wise in the nickel chloride solution at the same temperature (i.e. 65 °C) under vigorous stirring condition. The pH of the solution was measured with a portable pH meter (Orion 290 A) and found to be 8.6. The solution temperature was controlled by inserting manually adjustable thermocouple in the stirring pot. The reaction lasted for 4 h. After completing the reaction, greenish colored precipitates were obtained which was collected and washed with methanol and deionized water several times, then left to dry at room temperature. To prepare the NiO nanostructures, the as-grown products were calcined at 600 °C for 2 h. The as-grown and calcined products were structurally characterized by various analyses tools.

2.2. Characterizations

Detailed properties of the as-grown and calcined products were examined by using various analyses tools. The general morphologies of as-grown and calcined products were examined by the field emission scanning electron microscopy (FESEM), while the detailed structural properties of β - $\text{Ni}(\text{OH})_2$ nanoarchitectures were examined by the transmission electron microscopy (TEM) and high-resolution TEM (HRTEM). The crystal phase and crystallinity were analyzed by X-ray diffractometer (XRD) measured with $\text{Cu-K}\alpha$ radiations ($\lambda = 1.54178 \text{ \AA}$) in the range of 10–80° at 40 kV. The composition and quality of the synthesized flower-shaped β - $\text{Ni}(\text{OH})_2$ and NiO

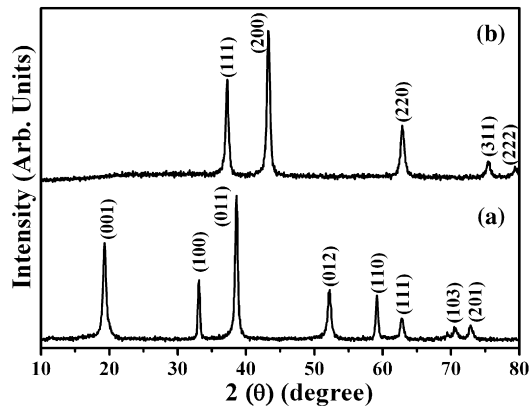


Fig. 1. Typical X-ray diffraction patterns of (a) as-grown β -Ni(OH)₂ and (b) NiO structures.

nanoarchitectures were characterized by Fourier transform infrared (FTIR) spectroscopy within the range of 4000–400 cm^{-1} wavenumbers. Thermogravimetric analysis (TGA) was performed on a TGA Q50 thermal analyzer in a flowing air atmosphere at the temperature range of 4–750 $^{\circ}\text{C}$ with a heating rate of 10 $^{\circ}\text{C}/\text{min}$.

3. Results and discussion

The crystallinity and crystal structures of the as-grown and calcined products were examined by X-ray diffraction (XRD) as shown in Fig. 1. In this Fig. 1(a), the typical XRD pattern of the as-grown β -Ni(OH)₂ products. All the diffraction peaks could be indexed as pure hexagonal structures β -Ni(OH)₂ with the cell constants of $a = 3.126 \text{ \AA}$ and $c = 4.662 \text{ \AA}$, which are well matched with the reported standard values (JCPDS card 74-2075). No other peaks for impurities such as α -Ni(OH)₂ or other phases are observed in the pattern confirming that the as-synthesized specimen is a single-crystalline pure β -Ni(OH)₂ phase. Moreover, the XRD pattern of the calcined products at 600 $^{\circ}\text{C}$ is shown in Fig. 1(b). The observed indexed peaks in this XRD pattern are fully matched with the corresponding pure cubic-structured crystalline NiO. Several peaks are observed in the pattern at $2\theta = 37.1^{\circ}$, 43.3° , 62.8° , 75.2° , and 79.3° assigned to the (111), (200), (220), (311) and (222) crystal planes, respectively. The indexed peaks are fully consistent with the cubic-structured crystalline NiO (JCPDS 47-1049) [8]. In addition to this, no peaks for any impurities such as α -Ni(OH)₂, β -Ni(OH)₂, or other phases were observed in the pattern which further confirm the crystalline and pure phase of the cubic NiO. Moreover, the observed peaks are sharper and higher in intensity which confirmed the well-crystallization of the obtained NiO structures.

Fig. 2(a)–(c) shows the general morphologies of the as-grown β -Ni(OH)₂ nanostructures. Large-quantity flower-like morphologies composed of thin nanosheet were obtained (Fig. 2(a) and (b)). The high-magnification SEM image shows that the nanosheets are connected to each other in such a manner that they form the network-like structures (figure (c)). The average dimensions of the observed nanosheets are in the range of 1.5–2 μm with the typical thickness of 50–70 nm. All the nanosheets are joined to each other in such a special fashion that the flowers exhibit spherical-shaped morphologies. Typically, the full array of a single flower-shaped structure is about 3–5 μm while the width ranges between 5 and 6 μm . Moreover, no breakage in nanosheets is observed from these flower-shaped β -Ni(OH)₂ structures.

Fig. 2(d) exhibits the typical TEM images of thin sheets of β -Ni(OH)₂ structures. As can be seen from the low-magnification TEM image that the nanosheets are transparent and constructed with Ni(OH)₂ nanofibers of $\sim 15 \text{ nm}$ in diameter and $\sim 400 \text{ nm}$ in length. It was also seen that some of the nanofibers are rolled to be needle-like structures. The HRTEM image of the corresponding nanosheet shown in Fig. 1(d) is demonstrated in the inset of (d). The HRTEM image clearly exhibits the distance between

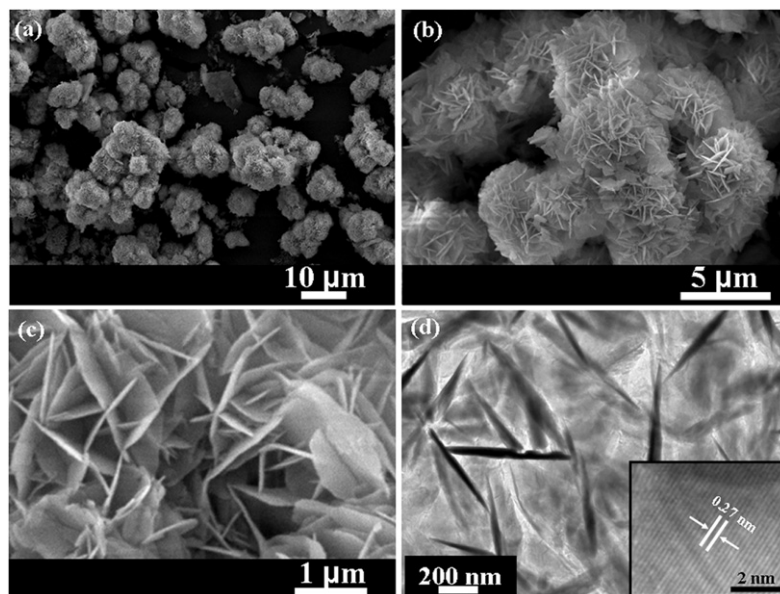


Fig. 2. Typical (a and b) low- and (c) high-magnification FESEM images; and (d) low- and (inset of (d)) high-resolution TEM images of the flower-shaped β -Ni(OH)₂ structures composed of thin-nanosheet networks prepared by simple solution process.

two lattice fringes, i.e. ~ 0.27 nm, which corresponds to the (01 $\bar{1}$ 0) crystal planes of β -Ni(OH)₂ [8]. The obtained HRTEM result is fully consistent with the XRD observations shown in Fig. 1(a).

Fig. 3(a) and (b) shows the low-magnification images of flower-shaped NiO structures obtained by calcination of as-grown β -Ni(OH)₂ samples at 600 °C in air. The general morphologies and dimensions of the obtained NiO products are almost similar to the initially grown flower-shaped β -Ni(OH)₂ structures. Fig. 3(c) exhibits the high-resolution FESEM image of the flower-shaped NiO structures. Some breakage in the nanosheet networks was observed from the outer surfaces of the flower-shaped NiO structures which most probably were due to the higher calcination temperature.

The quality and composition of the obtained structures were examined by FTIR spectroscopy in the range of 400–4000 cm⁻¹ and shown in Fig. 4. Fig. 4(a) shows the typical FTIR spectrum of as-synthesized flower-shaped β -Ni(OH)₂ nanostructures. A sharp and narrow peak at 3637 cm⁻¹ was observed, a characteristic peak for O–H stretching vibration, which confirms the brucite structure of β -Ni(OH)₂ phase [9]. The other peaks observed at 3450 cm⁻¹, 1633 cm⁻¹, are assigned to stretching vibration and bending vibration of adsorbed water molecules, respectively. The strong peak at 520 cm⁻¹ and small peak at 460 cm⁻¹ correspond to δ O–H of hydroxyl group and Ni–O stretching modes, respectively [9,10].

The typical FTIR spectrum of the flower-shaped NiO nanostructure is shown in Fig. 4(b) which exhibits the different composition from the parent Ni(OH)₂ sample. A sharp and strong peak at 3637 cm⁻¹ has been observed corresponding to OH stretching vibration. Moreover, two peaks at 536 and 460 cm⁻¹ were also observed which were related to the pure Ni–O stretching vibration.

The thermal behavior of flower-shaped β -Ni(OH)₂ nanostructures was examined with TGA measurement and shown in Fig. 5. From the TGA graph, it is seen that the β -Ni(OH)₂ started to decompose (weight loss) at about 285 °C. The major weight loss occurred rapidly between ~ 300 and ~ 340 °C. The total weight loss was measured to be about 20.1 % which is in a good agreement with the theoretical value (19.4%) calculated according to the following equation Ni(OH)₂(endothermic) \rightarrow NiO + H₂O [2]. Moreover, the TGA curve shows that there is no obvious weight loss when the temperature is higher than 580 °C and hence it can be concluded that β -Ni(OH)₂ nanostructures can be converted into NiO nanostructures at this temperature, as evident from the XRD observation shown in Fig. 1(b) which confirms the complete transformation of β -Ni(OH)₂ into crystalline cubic NiO.

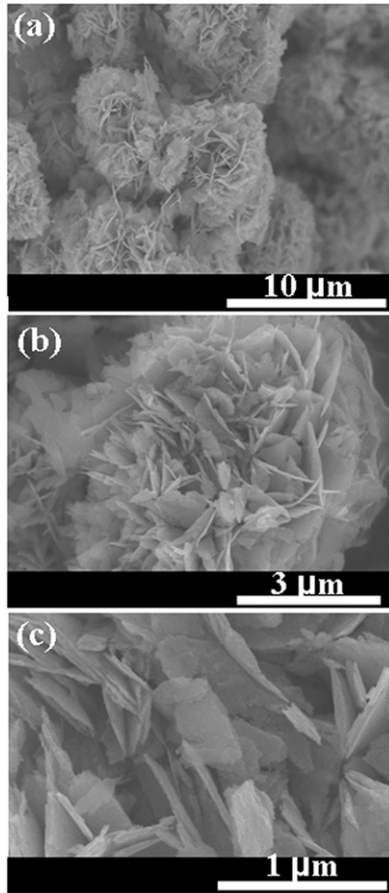


Fig. 3. (a) and (b) low-magnification and (c) high-resolution FESEM images of flower-shaped cubic NiO structures obtained by calcination of as-grown β -Ni(OH)₂ samples at 600 °C in air.

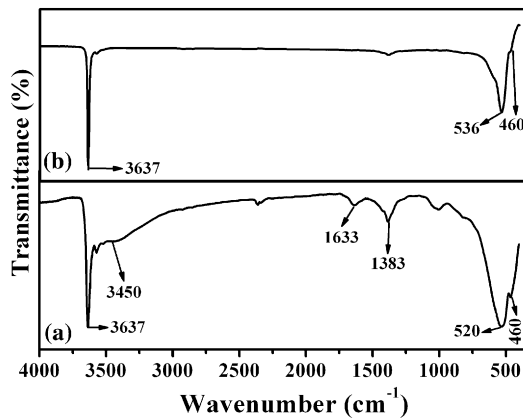


Fig. 4. Typical FTIR spectra for (a) as-synthesized flower-shaped β -Ni(OH)₂ and (b) calcined, flower-shaped NiO structures.

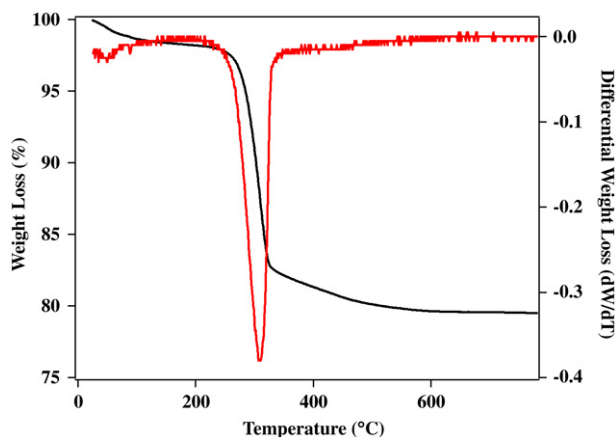


Fig. 5. TGA curve of the as-synthesized flower-shaped β -Ni(OH)₂ structures. The DTA curve for the same material is also shown confirming the phase transition from β -Ni(OH)₂ to NiO.

For the synthesis of Ni(OH)₂, ammonium hydroxide was slowly added in the aqueous solution of nickel chloride (NiCl₂) under continuous stirring at 65 °C. The typical chemical reaction for the formation of Ni(OH)₂ can be explained by a simple chemical equation: $\text{NiCl}_2 + 2\text{NH}_4\text{OH} \rightarrow \text{Ni(OH)}_2 + 2\text{NH}_4\text{Cl}$. The byproduct, ammonium chloride (NH₄Cl), was washed away after the reaction, by DI water and organic solvents. It is well known that the β -Ni(OH)₂ possesses a brucite-like (Mg(OH)₂) structure i.e. hexagonal lamellar structure, and hence have tendency to form 2D lamellar structure. Moreover, under normal precipitation conditions, these structures easily present the thin sheet-like morphologies with the sheet surfaces perpendicular to the *c*-axis, as sheets-like structures are thermodynamically stable along the *c*-axis direction [11]. Therefore, with prolonged reaction time, many Ni(OH)₂ nanosheets are joined to each other and form the nanosheet networks in the flower-shaped structures. Furthermore, the NiO were formed by the simple decomposition of Ni(OH)₂ into NiO according to the following equation: $\text{Ni(OH)}_2(\text{endothermic}) \rightarrow \text{NiO} + \text{H}_2\text{O}$ [2,11].

4. Conclusion

Simple aqueous solution route was employed to synthesize flower-shaped single-crystalline β -Ni(OH)₂ nanostructures composed of nanosheet networks in a large quantity at 65 °C in 4 h. Moreover, the conversion of β -Ni(OH)₂ into crystalline NiO was also obtained by calcination of the as-synthesized products at 600 °C. The FESEM images of these structures revealed that the flowers are composed of thin nanosheets which were connected to each other in such a manner that they form network-like morphologies. The as-prepared products were characterized in detail by XRD, FESEM, TEM, HRTEM, FTIR, and TGA techniques. The flowers with high-specific surface area are promising as positive electrode materials for alkaline rechargeable batteries. Moreover, these structures can also be used as a starting material for the synthesis of NiO nanostructures, versatile materials for the fabrication of catalysts, sensors, and electrochemical devices.

Acknowledgement

This work is supported by King Abdulaziz City for Science and Technology (KACST), Saudi Arabia.

References

- [1] J. Chen, D.H Bradhurst, S.X. Dou, H.K. Liu, J. Electrochem. Soc. 146 (1999) 3606.
- [2] X. Li, X. Zhang, Z. Li, Y. Qian, Solid State Commun. 137 (2006) 581.
- [3] M.M. Natile, A. Glisenti, Chem. Mater. 15 (2003) 2502.

- [4] T. Seto, H. Akinaga, F. Talano, K. Koga, T. Orii, M. Hirasawa, *J. Phys. Chem. B* 109 (2005) 13403.
- [5] P. Lunkenheimer, A. Loidl, C. Ottermann, H. Bange, *Phys. Rev. B* 44 (1991) 5927.
- [6] M. Cao, X. He, J. Chen, C. Hu, *Cryst. Growth Des.* 7 (2007) 170.
- [7] D. Chen, L. Gao, *Chem. Phys. Lett.* 405 (2005) 159.
- [8] D. Yang, R. Wang, M. He, J. Zhang, Z. Liu, *J Phys. Chem B.* 109 (2005) 7654.
- [9] L.X. Yang, Y.-J. Zhu, H. Tong, Z.H. Liang, L. Li, L. Zhang, *J. Sol. State Chem.* 180 (2007) 2095.
- [10] X.M. Liu, X.G. Zhang, S.Y. Fu, *Mater. Res. Bull.* 41 (2006) 620.
- [11] D. Wang, C. Song, Z. Hu, X. Fu, *J. Phys. Chem. B* 109 (2005) 1125.